HAL open science

Modulational instabilities in Josephson oscillations of elongated coupled condensates

Isabelle Bouchoule

To cite this version:

Isabelle Bouchoule. Modulational instabilities in Josephson oscillations of elongated coupled condensates. The European Physical Journal D : Atomic, molecular, optical and plasma physics, 2005, 35, pp.147. hal-00004203v3

HAL Id: hal-00004203

https://hal.science/hal-00004203v3

Submitted on 20 Jun 2005

HAL is a multi-disciplinary open access archive for the deposit and dissemination of scientific research documents, whether they are published or not. The documents may come from teaching and research institutions in France or abroad, or from public or private research centers.

L'archive ouverte pluridisciplinaire **HAL**, est destinée au dépôt et à la diffusion de documents scientifiques de niveau recherche, publiés ou non, émanant des établissements d'enseignement et de recherche français ou étrangers, des laboratoires publics ou privés.

EPJ manuscript No.
(will be inserted by the editor)

Modulational instabilities in Josephson oscillations of elongated coupled condensates

Isabelle Bouchoule

Laboratoire Charles Fabry de l'Institut d'Optique, UMR 8501 du CNRS, 91403 Orsay, France

the date of receipt and acceptance should be inserted later

Abstract. We study the Josephson oscillations of two coupled elongated condensates. Linearized calculations show that the oscillating mode uniform over the length of the condensates (uniform Josephson mode) is unstable : modes of non zero longitudinal momentum grow exponentially. In the limit of strong atom interactions, we give scaling laws for the instability time constant and unstable wave vectors. Beyond the linearized approach, numerical calculations show a damped recurrence behavior : the energy in the Josephson mode presents damped oscillations. Finally, we derive conditions on the confinement of the condensates to prevent instabilities.

PACS. 03.75.Lm Tunneling, Josephson effect, Bose-Einstein condensates in periodic potentials, solitons, vortices and topological excitations – 03.75.Kk Dynamic properties of condensates; collective and hydrodynamic excitations, superfluid flow

ccsd-00004203, version 3 - 20 Jun 2005

1 Introduction

Josephson oscillations arise between two Bose-Einstein condensates coupled by tunneling effect. They have been observed in superfluid Helium[1] and in superconductors[2] and have recently been achieved in dilute atomic BEC in a double well potential[3]. The physics of two coupled condensates has been extensively studied in a two modes model, where only two single particle modes are involved[4,5]. For atoms interacting in each well through a two-body interaction, different regimes are reached depending on the ratio between the tunneling strength to the interaction energy of atoms in each well[6,4]. For small interaction energy, one expects to observe Rabi oscillations. For large interaction energy one enters the Josephson regime. In this regime, oscillations around equilibrium configuration have a reduced amplitude in atom number and their frequency depends on the mean field energy. Finally, for very large interaction energy, quantum fluctuations are no longer negligible : the system is in the so called Fock regime and oscillations of atoms between the wells do not occur any more. In this paper, we assume this regime is not reached. Oscillations between the two wells, both in the Rabi and in the Josephson regime, are then well described by a mean field approach.

Atom chips[7] are probably good candidates to realize Josephson oscillations of Bose-Einstein Condensates as they enable the realization of micro-traps with strong confinement and flexible geometries. A possible configuration to realize a tunnel coupling between BEC on an atom-chip is proposed in [8]. In this proposal, the two condensates are very elongated and are coupled all along their longitudinal extension. With such an elongated geometry, both the Rabi and the Josephson regime could be accessed. However, in this case, tunnel coupling may be larger than the longitudinal frequency and the two modes model a priori breaks down. In this paper, we are interested in the stability of the uniform Josephson mode where all the atoms oscillate between the two wells independently of their longitudinal position. In the absence of interaction between atoms and if the transverse and longitudinal trapping potentials are separable, the longitudinal and transverse degree of freedom are decoupled and one expects to observe stable Rabi oscillations between the condensates. On the other hand interactions between atoms introduce non linearities that may couple the two motions. For a homogeneous situation such as atoms trapped in a box-like potential, uniform Josephson oscillations are a solution of the mean field evolution equations and are a priori possible, even in presence of interactions between atoms. However, the non linearities introduced by interactions between atoms may cause instability of this uniform Josephson mode. Similar modulational instabilities appear in many situations of nonlinear physics such as water waves propagation[9] or light propagation in a non linear fiber[11]. In the context of Bose Einstein condensates, they have been observed in presence of a periodic potential, at positions in the Brillouin zone where the effective mass is negative[12,13,14]. In our case a modulational instability would cause uniform Josephson oscillations to decay into modes of non vanishing longitudinal momentum. The goal of this paper is to investigate those instabilities.

We assume that all the relevant frequencies (interaction energy and tunnel coupling) are much smaller than the transverse oscillation frequencies in each well so that we can consider only a one dimensional problem. Thus, the system we consider is described by the Hamiltonian

$$\begin{aligned} H = \int dz \Big\{ & \tfrac{-\hbar^2}{2m}\left[\psi_1^\dagger(z)\tfrac{\partial^2}{\partial z^2}\psi_1(z) + \psi_2^\dagger(z)\tfrac{\partial^2}{\partial z^2}\psi_2(z)\right] \\ & + U(z)\left[\psi_1^\dagger(z)\psi_1(z) + \psi_2^\dagger(z)\psi_2(z)\right] \\ & + \tfrac{g}{2}\left[\psi_1^\dagger(z)\psi_1^\dagger(z)\psi_1(z)\psi_1(z) + \psi_2^\dagger(z)\psi_2^\dagger(z)\psi_2(z)\psi_2(z)\right] \\ & - \gamma\left[\psi_1^\dagger(z)\psi_2(z) + \psi_2^\dagger(z)\psi_1(z)\right]\Big\}, \end{aligned} \tag{1}$$

where g is the one-dimensional coupling constant and $U(z)$ is the longitudinal trapping potential. For a harmonic transverse confinement for which $\omega_\perp \ll \hbar^2/(ma^2)$, we have $g = 2\hbar\omega_\perp a$, where a is the scattering length[15]. The parameter γ describes the tunnel coupling.

We are interested in the stability of uniform Josephson oscillations around the equilibrium configuration where the two condensates have the same phase and equal longitudinal density. In the sections 2-4, we consider a homogeneous configuration where $U(z) = 0$. In the sections 2 and 3, we calculate the linearized evolution of modes of non zero longitudinal momentum in the presence of uniform Josephson oscillations. In the section 2, we give results of a calculation valid both in the Josephson and in the Rabi regime. In section 3, we show that, in the Josephson regime, the system is well described by a modified Sine-Gordon equation. For small amplitude oscillations, we derive scaling laws for the instability time constant and the wave vectors of the growing modes. In section 4, we go beyond the previous linearized approaches and present numerical results. We observe damped oscillations of the uniform Josephson mode amplitude. Such oscillations are similar to the Fermi-Pasta-Ulam recurrence behavior[16,17]. In the last section (5), we present numerical calculations in the case of a harmonic longitudinal confinement. We show that Josephson oscillations are stable for a sufficiently strong confinement and we give an approximate condition of stability.

2 Numerical linearized calculation

To investigate whether Josephson oscillations are unstable with respect to longitudinal excitations, we use a linearized calculation around the time-dependent solution corresponding to uniform Josephson oscillations. Writing $\psi_1 = \varphi_1 + \delta\psi_1$ and $\psi_2 = \varphi_2 + \delta\psi_2$ with uniform (z-independent) $\varphi_{1,2}$, Eq.1 gives to zeroth order the coupled Gross-Pitaevski equations

$$\begin{aligned} i\hbar\frac{d}{dt}\varphi_1 &= g|\varphi_1|^2\varphi_1 - \gamma\varphi_2 + (\gamma - \rho_0 g)\varphi_1 \\ i\hbar\frac{d}{dt}\varphi_2 &= g|\varphi_2|^2\varphi_2 - \gamma\varphi_1 + (\gamma - \rho_0 g)\varphi_2 \end{aligned}. \tag{2}$$

We shifted the zero of energy by adding to the Hamiltonian a "chemical potential" term $\gamma - \rho_0 g$, where ρ_0 is the density of each condensate at equilibrium. We recover here the well known results established for a two modes model[4,5,6]. More precisely, writing $\varphi_1 = \sqrt{N_1/L}\, e^{i\theta_1}$ and $\varphi_2 = \sqrt{(N-N_1)/L}\, e^{i\theta_2}$ where L is the size of the system, Eq.2 implies that the conjugate variables $\theta_1 - \theta_2$ and $k = (N_1 - N_2)/2$ evolve according to the non rigid pendulum Hamiltonian $H_p = E_C k^2/2 + E_J\sqrt{1 - 4k^2/N^2}\cos(\theta_1 - \theta_2)$ where the charge energy is $E_c = 2g/L$ and the Josephson energy is $E_J = \gamma N$. We consider oscillations of $\theta_1 - \theta_2$ around 0 of amplitude Θ_{osc}. Let us now consider the evolution of excitations around those uniform oscillations. To first order in $\delta\psi_{1,2}$, Eq.1 yields the coupled Bogoliubov equations

$$i\hbar\frac{d}{dt}\begin{pmatrix} \delta\psi_1 \\ -\delta\psi_1^+ \\ \delta\psi_2 \\ -\delta\psi_2^+ \end{pmatrix} = \begin{pmatrix} \mathcal{L}_1 & \mathcal{C} \\ \mathcal{C} & \mathcal{L}_2 \end{pmatrix}\begin{pmatrix} \delta\psi_1 \\ -\delta\psi_1^+ \\ \delta\psi_2 \\ -\delta\psi_2^+ \end{pmatrix} \tag{3}$$

where, for $i = 1, 2$,

$$\mathcal{L}_i = \begin{pmatrix} -\frac{\hbar^2}{2m}\frac{\partial^2}{\partial z^2} + 2g|\varphi_i|^2 - \rho_0 g + \gamma & -g\varphi_i^2 \\ g\varphi_i^{*2} & \frac{\hbar^2}{2m}\frac{\partial^2}{\partial z^2} - 2g|\varphi_i|^2 + \rho_0 g - \gamma \end{pmatrix} \tag{4}$$

and the coupling term is

$$\mathcal{C} = \begin{pmatrix} -\gamma & 0 \\ 0 & \gamma \end{pmatrix}. \tag{5}$$

Instabilities arise if there exist modes growing exponentially in time under Eq.3. The evolution matrix is invariant under translation so that we can study independently plane waves modes $e^{ikz}(u_1, v_1, u_2, v_2)$, the second derivatives

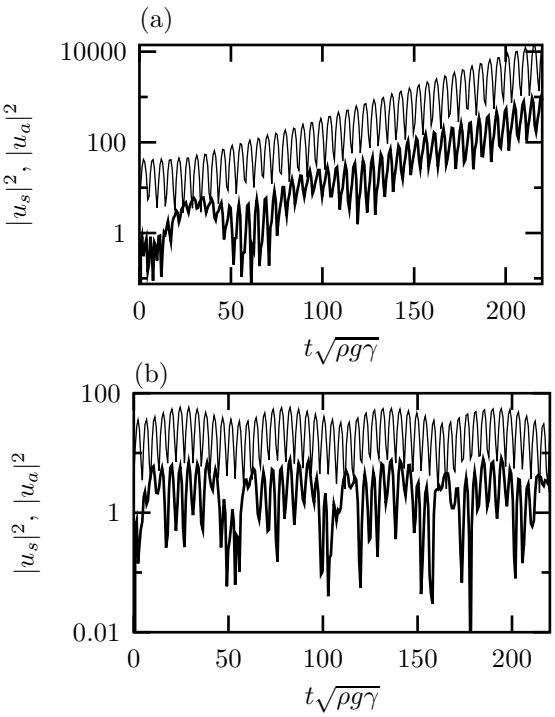

Fig. 1. *Evolution of the square amplitude of the symmetric (fat lines) and antisymmetric (thin lines) excitations of wave vector* $k = 0.1\sqrt{m\rho_0 g}/\hbar$ *(a) and* $k = 0.3\sqrt{m\rho_0 g}/\hbar$ *(b). Those graphs are computed for* $\gamma = 0.1\rho_0 g$ *and a uniform Josephson oscillation amplitude* $\Theta_{osc} = 0.6$.

in $\mathcal{L}_1$ and $\mathcal{L}_2$ being replaced by $-k^2$. Note that the evolution of excitations depends only on the four parameters k, $\rho_0 g$, γ and Θ_{osc}. For a given k component, we numerically evolve equations 2 and 3. Fig.1 gives the evolution of the square amplitude of the symmetric mode $|u_s|^2 = |u_1 + u_2|^2$ and of the antisymmetric mode $|u_a|^2 = |u_1 - u_2|^2$ for two different k vectors, for $\gamma = 0.1\rho_0 g$ and for $\Theta_{osc} = 0.6$. For these calculations, we choose the initial condition as $(u_1, v_1, u_2, v_2) = (1, -1, -1, 1)$. In the two cases, we observe a fast oscillation at a frequency close to the frequency of the antisymmetric mode $\sqrt{(2\rho_0 g + 2\gamma + \hbar^2k^2/2m)(2\gamma + \hbar^2k^2/2m)}$ and a slower oscillation at a frequency close to that of the symmetric mode $\sqrt{(2\rho_0 g + \hbar^2k^2/2m)\hbar^2k^2/2m}$[18]. On top of this, we observe, for $k = 0.1$, an exponential growth $e^{2\Gamma t}$ of $|u_1+u_2|^2$ and $|u_1-u_2|^2$, signature of an unstability. We find that, for given $\rho_0 g$ and Θ_{osc}, the instability domain in k is $[0, k_{max}]$. Fig.2 gives the maximum growth rate Γ and the maximum unstable wave vector k_{max}.

3 Calculation in the Josephson limit

In this section, we focus on the Josephson regime where $\gamma \ll \rho_0 g$[10]. In this regime the amplitude of oscillations in the relative density $\delta\rho$ remains small compared to the mean density and one can assume $\rho_1 = \rho_2$ in the Josephson energy term of the Hamiltonian. Furthermore, we restrict ourselves to long wavelength excitations described by phonons and we neglect anharmonicity of phonons. Then, the Hamiltonian reduces to

$$H_J = H_s + H_{SG} + H_c, \tag{6}$$

where, writing $\psi_1 = \sqrt{\rho_1}e^{i\theta_1}$, $\psi_2 = \sqrt{\rho_2}e^{i\theta_2}$, $\theta_a = \theta_1 - \theta_2$, $\theta_s = \theta_1 + \theta_2$, $\rho_a = (\rho_1 - \rho_2)/2$ and $\rho_s + \rho_0 = (\rho_1 + \rho_2)/2$,

$$H_s = \int \left(\frac{\hbar^2\rho_0}{4m} \left(\frac{\partial\theta_s}{\partial z} \right)^2 + g\rho_s^2 \right) dz \tag{7}$$

describes the symmetric phonons,

$$H_{SG} = \int \left(\frac{\hbar^2\rho_0}{4m} \left(\frac{\partial\theta_a}{\partial z} \right)^2 + g\rho_a^2 - 2\gamma\rho_0(\cos(\theta_a) - 1) \right) dz \tag{8}$$

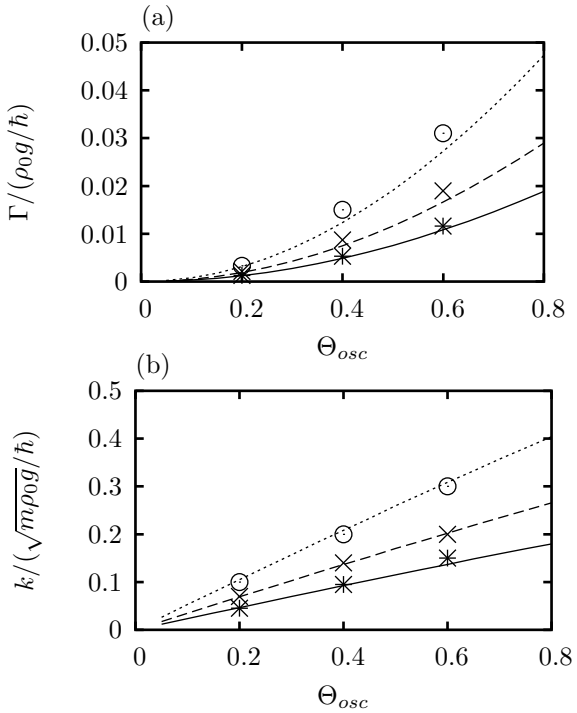

Fig. 2. *Maximum instability rate of excitations (a) and maximum wave vector k of unstable modes (b) as a function of the amplitude of the relative phase oscillations for $\gamma = 0.05\rho_0 g$ (stars and solid line) $\gamma = 0.1\rho_0 g$ (crosses and dashed line) and $\gamma = 0.2\rho_0 g$ (circles and dotted line). The points are the results of the linearized numerical calculations presented in section 2 and are given with a precision of 10%. The continuous lines are given by diagonalising the four by four matrix as presented in section 3.*

is the Sine-Gordon Hamiltonian and

$$H_c = -2\gamma \int \rho_s(\cos(\theta_a) - 1)dz \tag{9}$$

is a coupling between the symmetric and antisymmetric modes. The Sine-Gordon Hamiltonian has already been introduced in the physics of elongated supraconducting Josephson junction[2]. In those systems, symmetric modes would have a very large charge and magnetic energy and do not contribute. The Sine-Gordon model has been extensively studied[19]. In particular, it has been shown that, for a Sine-Gordon Hamiltonian, oscillations of well defined momentum (in particular $k = 0$) present Benjamin-Feir instabilities[19]. Our system is not described by the Sine-Gordon Hamiltonian because of the presence of H_c. In the following, we derive results about stability of our modified Sine-Gordon system. As we will see later, we recover results close to that obtained for the Sine-Gordon model.

The Josephson oscillations correspond to oscillations where $\rho_a = \rho_{osc}$ and $\theta_a = \theta_{osc}$ are independent of z. They are given by

$$\begin{cases} \dfrac{\partial \rho_{osc}}{\partial t} = 2\gamma\rho_0 \sin(\theta_{osc})/\hbar \\ \dfrac{\partial \theta_{osc}}{\partial t} = -2g\rho_{osc}/\hbar \end{cases} \tag{10}$$

They also induce an oscillation $\theta_{osc}^{(s)}$ of θ_s given by

$$\frac{\partial \theta_{osc}^{(s)}}{\partial t} = -2\gamma\left(\cos(\theta_{osc}) - 1\right)/\hbar. \tag{11}$$

To investigate whether some non vanishing k modes are unstable in presence of a Josephson oscillation, we linearize, as in the previous section, the equation of motion derived from Eq.6 around the solution ρ_{osc}, θ_{osc}. Because of translational invariance, we can study independently the evolution of modes of well defined longitudinal wave vector k. Writing $\rho_1 = \rho_0 + \rho_{osc} + (\delta\rho_a + \delta\rho_s)e^{ikz}$, $\rho_2 = \rho_0 - \rho_{osc} + (-\delta\rho_a + \delta\rho_s)e^{ikz}$, $\theta_1 = (\theta_{osc}^{(s)} + \theta_{osc} + (\delta\theta_s + \delta\theta_a)e^{ikz})/2$, and

$\theta_2 = (\theta_{osc}^{(s)} - \theta_{osc} + (\delta\theta_s - \delta\theta_a)e^{ikz})/2$, we find the evolution equation

$$\hbar\frac{d}{dt}\begin{pmatrix}\delta\rho_a/\rho_0\\ \delta\theta_a\\ \delta\rho_s/\rho_0\\ \delta\theta_s\end{pmatrix} = \begin{pmatrix} 0 & -\frac{\hbar^2k^2}{2m}+2\gamma\cos(\theta_{osc}) & 2\gamma\sin(\theta_{osc}) & 0\\ -2\rho_0 g & 0 & 0 & 0\\ 0 & 0 & 0 & -\frac{\hbar^2k^2}{2m}\\ 0 & 2\gamma\sin(\theta_{osc}) & -2\rho_0 g & 0\end{pmatrix}\begin{pmatrix}\delta\rho_a/\rho_0\\ \delta\theta_a\\ \delta\rho_s/\rho_0\\ \delta\theta_s\end{pmatrix}. \tag{12}$$

We solved numerically Eq.10 and Eq.12 and we find that modes of low k wave vectors are unstable. Fig.3 gives the instability rate and the maximum k wave vector of unstable modes. Those results agree within 10% to the more general results of the previous section as long as $\gamma/\rho_0 g < 0.2$ and the oscillation amplitude fulfills $\Theta_{osc} < 0.6$.

To get more insight into the physics involved and to obtain scaling laws for the instability rate and the instability range in k, we will perform several approximations. The evolution matrix M of Eq.12 is periodic in time with a period ω_J. We can thus use a Floquet analysis[20] and look for solutions of Eq.12 in the form

$$e^{i\nu t}\sum_{n=-\infty}^{+\infty} e^{in\omega_J t}c_n = e^{i\nu t}\sum_{n=-\infty}^{+\infty} e^{in\omega_J t}\begin{pmatrix}c_{1n}\\ c_{2n}\\ c_{3n}\\ c_{4n}\end{pmatrix}. \tag{13}$$

Expanding Eq.12 for each Fourier component, we find

$$\nu c_n = -\omega_J n c_n - iM_0 c_n - i\sum_m M_m c_{n-m}, \tag{14}$$

where the time independent matrices M_n are the Fourier components

$$M_m = \frac{\omega_J}{2\pi\hbar}\int_0^{\frac{2\pi}{\omega_J}} e^{-im\omega_J t}M(t)dt \tag{15}$$

Thus, solutions of Eq.12 are found as eigenvalues of the linear set of equations (14). The mode is unstable if there exists an eigenvalue of non vanishing real part and its growth rate is the real part of the eigenvalue.

For $\Theta_{osc} = 0$, only the dc component M_0 is not vanishing and its eigenvalues are $\pm\omega_a = \pm i\sqrt{2\rho_0 g(2\gamma + \hbar k^2/2m)}$ and $\pm\omega_s = \pm i\hbar k\sqrt{\rho_0 g/m}$ corresponding, for each Fourier component n, to the symmetric modes $c_{\pm\ n}^{(s)}$ and antisymmetric modes $c_{\pm\ n}^{(a)}$. The four states $c_{-\ -1}^{(a)}$, $c_{-\ 0}^{(s)}$, $c_{+\ 0}^{(s)}$ and $c_{+\ 1}^{(a)}$ form a subspace almost degenerate in energy and of energy far away from the other states as depicted Fig.4. Thus, we will restrict ourselves to those states in the following. In the limit of oscillations of small amplitude Θ_{osc}, the matrix elements of M can be expanded to second order in θ_{osc}. Furthermore, the oscillations are well described by $\theta_{osc} = \Theta_{osc}\cos(\omega_J t)$, where $\omega_J = 2\sqrt{\gamma\rho_0 g}(1-\Theta_{osc}^2/16)/\hbar$. We then find that, in the 4 dimensional subspace spanned by ($c_{-\ -1}^{(a)}$, $c_{-\ 0}^{(s)}$, $c_{+\ 0}^{(s)}$,$c_{+\ 1}^{(a)}$), the eigenvalue ν of Eq.14 are the eigenvalues of the four by four matrix

$$\mathcal{M} = \begin{pmatrix} i(-\omega_a+\omega_J+\gamma\Theta_{osc}^2 f_a^2/4) & -i\gamma\Theta_{osc}f_a/(2f_s) & \gamma\Theta_{osc}f_a/(2f_s) & -\gamma\Theta_{osc}^2 f_a^2/8\\ i\gamma\Theta_{osc}f_a/f_s/2 & i\omega_s & 0 & -\gamma\Theta_{osc}f_a/(2f_s)\\ {}_{\gamma}\Theta_{osc}f_a/(2f_s) & 0 & -i\omega_s & -i\gamma\Theta_{osc}f_a/(2f_s)\\ -\gamma\Theta_{osc}^2 f_a^2/8 & \gamma\Theta_{osc}f_a/(2f_s) & i\gamma\Theta_{osc}f_a/(2f_s) & i(\omega_a-\omega_J-\gamma\Theta_{osc}^2 f_a^2/4)\end{pmatrix} \tag{16}$$

where $f_a = (2\rho_0 g/(\hbar^2k^2/2m + 2\gamma))^{(1/4)}$ and $f_s = (4m\rho_0 g/\hbar^2k^2)^{(1/4)}$.

We numerically diagonalise this matrix and find the instability rate as the largest real part of the eigenvalues. For a given oscillation amplitude Θ_{osc}, scanning the wave vector k, we find the largest instability rate and the maximum wave vector of unstable modes. Fig.3 compare those results with the values obtained by integration of Eq.12. We find a very good agreement in the range $\theta < 0.6$ and $\gamma/\rho_0 g < 0.1$. Finally, in Fig.2, we compare the instability rate and the maximum unstable wave vector found with this simplified Floquet analysis with the more general results of section 1. We find a very good agreement as long as $\gamma/\rho_0 g < 0.2$ and $\Theta_{osc} < 0.6$.

If we restrict ourselves to terms linear in Θ_{osc}, then the only effect of the Josephson oscillations is to introduce a coupling between the symmetric and antisymmetric mode. We checked that this coupling alone does not introduce any

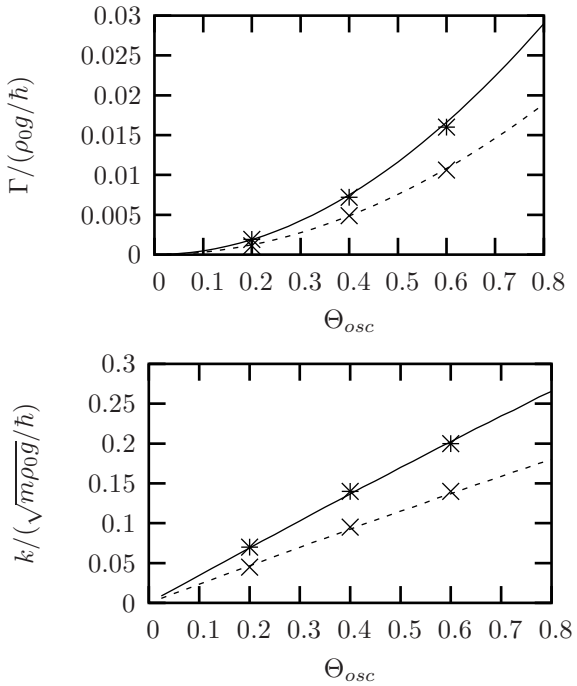

Fig. 3. *Comparison between numerical evolution of Eqs.10 and 12 (points) and the results obtained by diagonalising the 4 by 4 matrix of the Floquet representation (lines). Parameters are $\gamma = 0.1 \times \rho_0 g$ (stars and continuous lines) and $\gamma = 0.05 \times \rho_0 g$ (crosses and dashed line).*

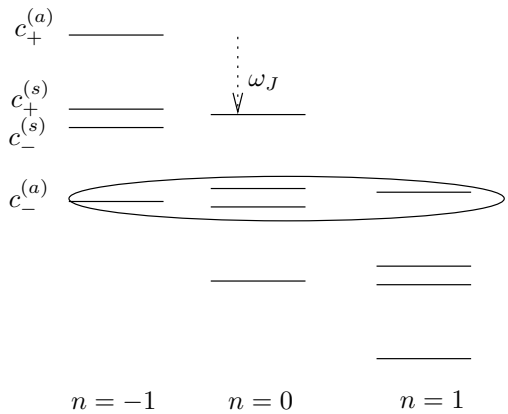

Fig. 4. *Floquet representation of the equation Eq.12. The ellipse surrounds the four states that are considered in the calculation of instability rates.*

instability. Thus instability is due to the quadratic terms. Those terms contain a modulation at $2\omega_J$. This modulation corresponds to the modulation of the frequency of the antisymmetric mode

$$\omega_a^2 = 2\rho_0 g(\hbar^2 k^2/2m + 2\gamma - 2\gamma\Theta_{osc}^2/4) + \gamma\rho_0 g\Theta_{osc}^2 \cos(2\omega_J t). \tag{17}$$

This parametric oscillation leads to instability for $k \in [0, \Theta_{osc}\sqrt{m\gamma/2}/\hbar]$ and the instability time constant at resonance is $\Gamma = \Theta_{osc}^2 \frac{\sqrt{\gamma\rho_0 g}}{8\hbar}$. We recover here the well known results of Benjamin-Feir instability derived for example in [19] using the multiple-scale perturbation technique. In our case, the coupling to the symmetric mode will modify those values. However, for small values of γ, the qualitative behavior is unchanged. Indeed, as seen in Fig.5, as long as $\gamma < 0.05\rho_0 g$ and within a precision of 10%, the instability rate Γ scales as

$$\Gamma = 0.122(1)\Theta_{osc}^2\sqrt{\gamma\rho_0 g}/\hbar \tag{18}$$

and the maximum wave vector of unstable modes as

$$k_{max} = 0.97(1)\frac{\sqrt{m\gamma}}{\hbar}\Theta_{osc}. \tag{19}$$

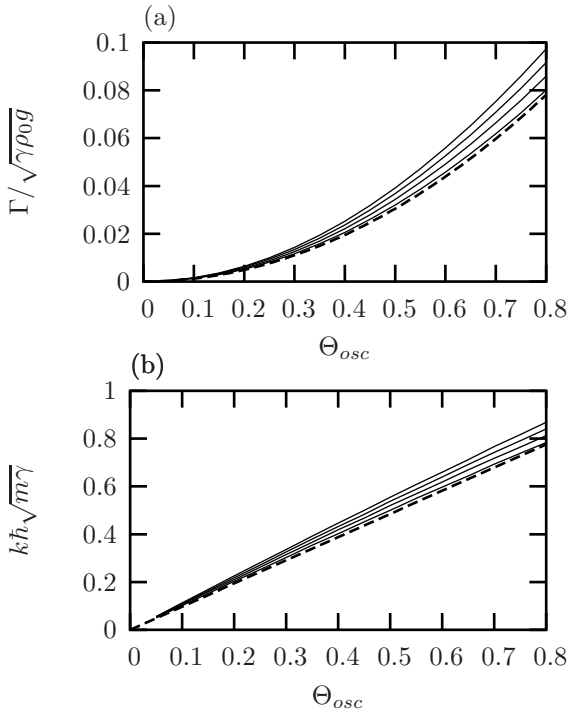

Fig. 5. Maximum instability rate normalized to the Josephson oscillation frequency (a) and maximum wave vector of unstable modes normalized to $\sqrt{m\gamma}/\hbar$ (b) as a function of the oscillations amplitude Θ_{osc} for different ratios $\gamma/\rho_0 g$ (from lower curves to upper curves : 0.02,0.06,0.1,0.14). Fat dashed lines are the scaling laws Eq.18 and 19. Thin continuous lines are found by diagonalising the matrix of Eq.16.

For larger γ, the Γ and k_{max} are higher than those lows as seen in Fig.5.

4 Beyond the linearisation

The two previous sections give a linearized analysis of the evolution of perturbations. They show that the presence of uniform Josephson oscillations produces instabilities of modes of non vanishing momentum. The energy in these mode grows and consequently, the energy of the uniform Josephson mode decreases and one expects a decrease of the uniform Josephson oscillations amplitude. Such a decrease is beyond the previous linearized analysis and we perform full numerical calculation of the evolution of the mean fields $\psi_1(z,t)$ and $\psi_2(z,t)$. The evolution equations derived from Eq.1 are

$$\begin{cases} i\hbar\dfrac{d}{dt}\psi_1 = -\dfrac{\hbar^2}{2m}\dfrac{d^2\psi_1}{dz^2} + g|\psi_1|^2\psi_1 - \gamma\psi_2 \\ i\hbar\dfrac{d}{dt}\psi_2 = -\dfrac{\hbar^2}{2m}\dfrac{d^2\psi_2}{dz^2} + g|\psi_2|^2\psi_2 - \gamma\psi_1 \end{cases} \tag{20}$$

Fig.6 gives the evolution of the total number of atoms in the condensate 1, $N_1 = \int |\psi_1|^2$, for initial amplitude $\Theta_{osc} = 0.6$ and for different values of $\gamma/(\rho_0 g)$. For these calculations, the initial state consists in a z-independent phase difference Θ_{osc} between ψ_1 and ψ_2 superposed on thermal fluctuations of the density and phase of the two condensates corresponding to a temperature $k_B T = \rho_0 g/10$. We observe that the amplitude of the Uniform Josephson Oscillations presents damped oscillations. For $\gamma \ll \rho_0 g$, the period of these amplitude oscillations is about three times the inverse of the instability rate of Eq.18. The ratio between the Josephson frequency and the frequency of these amplitude oscillations is about 20 and is almost independent on the ratio between γ and $\rho_0 g$ as long as $\gamma < \rho_0 g$. For larger γ, this ratio increases and more Josephson oscillations are seen in a period of the amplitude modulation. Such amplitude oscillations are a reminiscence of the Fermi-Ulam-Pasta recurrence behavior observed in many non linear systems with modulational instabilities[19,16,17]. In particular, this recurrence behavior has been seen in numerical evolution of the Sine-Gordon Hamiltonian[21]. In our case, we observe an additional damping which results probably from the coupling to symmetric modes.

The case of an initial amplitude $\Theta_{osc} = \pi/2$ is of particular interest as, in absence of interactions between atoms, it corresponds to Rabi oscillations of maximum amplitude. Fig.7 gives the evolution of N_1 for $\gamma = \rho_0 g$ and an initial amplitude $\Theta_{osc} = \pi/2$.

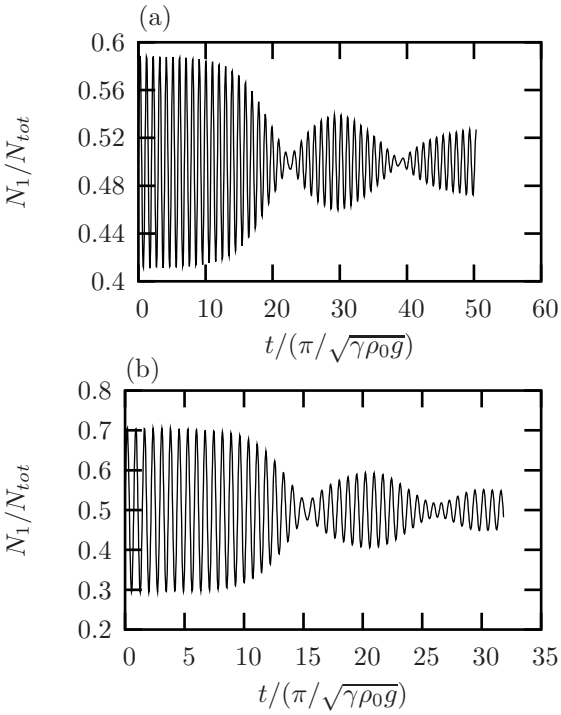

Fig. 6. *Evolution of the number of atoms in the condensate 1, normalized to the total number of atoms, as a function of time. The initial state corresponds to a phase difference between the condensate $\Theta_{osc} = 0.6$ superimposed on phase and density fluctuations corresponding to a thermal equilibrium at temperature $k_B T = 0.1\rho_0 g$. For this calculation, $\gamma = 0.1\rho_0 g$ (a) and $\gamma = \rho_0 g$ (b).*

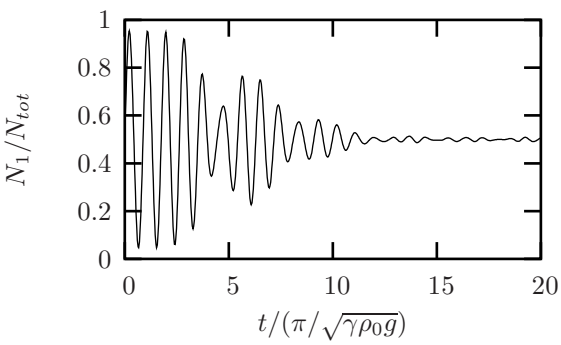

Fig. 7. *Evolution of the number of atoms in the condensate 1, normalized to the total number of atoms, as a function of time for $\gamma = \rho_0 g$ and an initial phase difference between condensates $\Theta_{osc} = \pi/2$. Initial thermal population of excited modes corresponding to $k_B T = 0.1\rho_0 g$ is assumed.*

5 Case of a confined system

In the previous sections, we considered large and homogeneous systems. We found that unstable excited modes are those of low wave vectors. In the Josephson limit where $\gamma \ll \rho_0 g$, we derived the scaling law Eq.19 for the maximum unstable wave vector. In a cloud trapped in a box like potential of extension L, the minimum k value of the excitation modes is $2\pi/L$. Thus, if

$$L < \frac{2\pi\hbar}{1.0\sqrt{m\gamma}\Theta_{osc}}, \tag{21}$$

the minimum wave vector of excited modes is larger than the maximum unstable k value Eq.19 and the system is stable. This condition can be understood in a different way : the energy of the lowest longitudinal mode is $\hbar 2\pi\sqrt{\rho_0 g}/(mL)$ (here we assume $L \gg \hbar/\sqrt{m\rho_0 g}$). Thus, we find that the system is stable provided that the energy of the lowest excited mode satisfies $E_{exc} > 0.52\omega_J\Theta_{osc}$ where $\omega_J = 2\sqrt{\gamma\rho_0 g}/\hbar$ is the Josephson frequency.

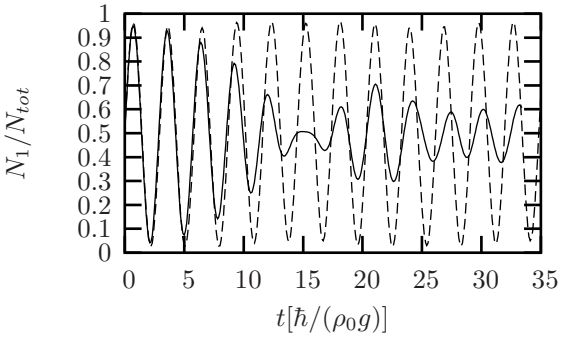

Fig. 8. Josephson oscillations of clouds trapped in a harmonic potential of frequency $\omega = 0.1\rho_0 g/\hbar$ (solid line) and $\omega = \rho_0 g/\hbar$ (dashed line), where ρ_0 is the peak linear density in each condensate. The initial phase difference between the condensates is $\pi/2$ and the tunnel coupling is $\gamma = \rho_0 g$. N_1 is the number of atoms in the condensate 1 and N_{tot} the total number of atoms.

An approximate condition of stability of Josephson oscillations in the case of a cloud trapped in a harmonic longitudinal potential of frequency ω is found as follows. The size of cloud, described by a Thomas Fermi profile, is $L = 2\mu/(m\omega^2)$, where $\mu = \rho_0 g$ is the chemical potential and ρ_0 the peak linear density. Then, from the same argument as above, one expects to observe stable oscillations for

$$\omega > \alpha\sqrt{\gamma\rho_0 g}\Theta_{osc} = \alpha\Theta_{osc}\omega_J/2 \tag{22}$$

where α is a numerical factor close to one. We performed numerical simulations of the evolution in the case of a harmonic potential, adding to both left hand sides of Eqs.20 a trapping potential $1/2m\omega^2 z^2$. The initial situation is the Thomas Fermi profile superposed on thermal random fluctuations and a global phase difference between the condensates $\Theta_{osc} = \pi/2$. The tunnel coupling is $\gamma = \rho_0 g$. The resulting Josephson oscillations are shown in Fig.8 for $\omega = \rho_0 g/\hbar$ and $\omega = 0.1\rho_0 g/\hbar$. We observe that for $\omega = \rho_0 g/\hbar$, Josephson oscillations are stable whereas, for $\omega = 0.1\rho_0 g/\hbar$, oscillations are unstable.

6 Conclusion and prospects

We have shown that Josephson oscillations of two coupled elongated condensates are unstable with respect to excitations of longitudinal modes. The unstable modes are those of small wave vectors. In the Josephson limit where $\gamma \ll \rho_0 g$, we have derived the scaling lows Eq.18 and Eq.19 for the instability time constant and wave vectors. Since the frequency of Josephson oscillations are $2\sqrt{\gamma\rho_0 g}$, the first equation tells us that the number of oscillations that can be observed scales as Θ_{osc}^2 and is independent on $\gamma/\rho_0 g$. This is true as long as $\gamma < \rho_0 g$. For larger $\gamma/(\rho_0 g)$, the Josephson condition is not fulfilled. Effect of interactions is less pronounced and more oscillations can be observed. Performing numerical calculations beyond the linearized approach, we have shown that the system presents a recurrence behavior, although it is damped quickly. Finally, we investigated the stability of oscillations in finite size systems. Eq.21 gives the maximum longitudinal size of confined condensate that enables the presence of stable Josephson oscillations. We also considered the case of harmonically trapped cloud and give an approximate condition on the oscillation frequency to have stable Josephson oscillations.

The results of this paper are not changed drastically for finite temperature. Indeed, although elongated Bose-Einstein condensates present thermally excited longitudinal phase fluctuations[22,23], it has been shown in [18] that, because the antisymmetric modes present an energy gap, thermal fluctuations of the relative phase between elongated coupled condensates are strongly suppressed.

Among the possible extensions of this work, two questions are of immediate experimental interest. First, the effect of a random longitudinal potential could be investigated. Indeed, it has been proposed to realized elongated coupled condensates using magnetic trapped formed by micro-fabricated wires[8], but, for such systems, a roughness of the longitudinal potential has been observed[24,25,26]. If the amplitude of the roughness potential is smaller than the chemical potential of the condensate, one expects to still have a two single elongated condensate. However, the roughness of the potential may change significantly the results of this paper. Second, the effect of correlations between atoms may be studied. Indeed, for large interactions between atoms, correlations between atoms become important. More precisely, for $\rho_0 < mg/\hbar^2$, a mean field approach is wrong and the gas is close to the Tonks-Girardeau regime[27, 28,29]. Such a situation is not described in this paper in which a mean field approach has been assumed. Thus, a new study should be devoted to the physics of coupled elongated Tonks gas.

Dynamical instabilities of the uniform Josephson mode are not the only effect of non linearities in the system of two coupled elongated condensates and other interesting phenomena are expected. For instance, ref.[30] shows that Josephson vortices similar to the solitons of the Sine-Gordon model exist for large enough interaction energy.

We thank Dimitri Gangardt for helpful discussions. This work was supported by EU (IST-2001-38863, MRTN-CT-2003-505032), DGA (03.34.033) and by the French ministery of research (action concertée "nanosciences").

References

1. S. V. Pereverzev *et al.*, Nature **388**, 449 (1997).
2. K. K. Likharev, *Dynamics of Josephson junctions and circuits* (Gordon and Breach science publishers, 1986).
3. M. Albiez *et al.*, cond-mat/0411757 (2004).
4. A. J. Legett, Rev. Mod. Phys. **73**, 307 (2001).
5. F. Sols in *Bose-Einstein Condensation in Atomic Gases*, IOS Press (1999)
6. A. Smerzi, S. Fantoni, S. Giovanazzi, and S. R. Shenoy, Phys. Rev. Lett. **79**, 4950 (1997).
7. R. Folman *et al.*, Adv. Atom. Mol. Opt. Phys. **48**, 263 (2002), and references therein.
8. J. Estève, T. Schumm, J.B. Trebbia, I. Bouchoule, A. Aspect, C.I. Westbrook, Eur. Phys. J. D (2005,d05098)
9. T. B. Benjamin and J. E. Feir, J. Fuid Mech. **27**, 417 (1967).
10. We also consider that $\gamma \gg g\rho_0/N^2$, N being the total number of atoms, so that quantum fluctuations of the relative phase are negligible.
11. K. Tai, A. Hasegawa, and A. Tomita, Phys. Rev. Lett. **49**, 236 (1986).
12. L. Fallani *et al.*, Phys. Rev. Lett. **93**, 140406 (2004).
13. B. Wu and Q. Niu, Phys. Rev. A **64**, 061603 (2001).
14. V. V. Konotop and M. Salerno, Phys. Rev. A **65**, 021602 (2002).
15. M. Olshanii, Phys. Rev. Lett. **81**, 938 (1998).
16. H. C. Yuen and W. E. Ferguson, Phys. Fluids **21**, 1275 (1978).
17. E. Infeld, Phys. Rev. Lett. **47**, 717 (1981).
18. N. K. Whitlock and I. Bouchoule, Phys. Rev. A **68**, 053609 (2003).
19. A. C. Newell, *Solitons in Mathematics and Physics* (Society of Industrial and Applied Mathematics, ADDRESS, 1985), p.43.
20. J. H. Shirley, Phys. Rev. **138**, B979 (1965).
21. D. Barday and M. Remoissenet, Phys. Rev. B **43**, 7297 (1991).
22. S. Dettmer *et al.*, Phys. Rev. Lett. **87**, 160406 (2001).
23. S. Richard, F. Gerbier, J. H. Thywissen, M. Hugbart, P. Bouyer and A. Aspect, cond-mat/0303137
24. J. Fortágh *et al.*, Phys. Rev. A **66**, 41604 (2002).
25. M. P. A. Jones *et al.*, J. Phys. B: At. Mol. Opt. Phys. **37**, L15 (2004).
26. J. Estève *et al.*, Phys. Rev. A **70**, 043629 (2004).
27. P. B. *et al.*, Nature **429**, 277 (2004).
28. H. Moritz, T. Stöferle, M. Köhl, and T. Esslinger, Phys. Rev. Lett. **91**, 250402 (2003).
29. B. L. Tolra *et al.*, Phys. Rev. Lett. **92**, 190401 (2004).
30. V. M. Kaurov and A. B. Kuklov, Phys. Rev. A **71**, 011601 (2004)